Appl Microbiol Biotechnol (2006) 72: 361–367
DOI 10.1007/s00253-005-0263-8

Thomas K. Wood · Andrés F. González Barrios · Moshe Herzberg · Jintae Lee

Motility influences biofilm architecture in *Escherichia coli*

Received: 27 June 2005 / Revised: 9 November 2005 / Accepted: 13 November 2005 / Published online: 6 January 2006

Abstract Eight *Escherichia coli* strains were studied in minimal medium with a continuous flow system using confocal microscopy. K12 wild-type strains ATCC 25404 and MG1655 formed the best biofilms (~43 μm thick, 21 to 34% surface coverage). JM109, DH5α, and MG1655 *motA* formed intermediate biofilms (~13 μm thick, 41 to 58% surface coverage). BW25113, MG1655 *qseB*, and MG1655 *fliA* had poor biofilms (surface coverage less than 5%). The best biofilm-formers, ATCC 25404 and MG1655, displayed the highest motility, whereas the worst biofilm former, BW25113, was motility-impaired. The differences in motility were due to differences in expression of the motility loci *qseB*, *flhD*, *fliA*, *fliC*, and *motA* (e.g., *qseB* expression in MG1655 was 139-fold higher than BW25113 and 209-fold higher than JM109). Motility affected the biofilm architecture as those strains which had poor motility (*E. coli* JM109, *E. coli* MG1655 *motA*, and DH5α) formed flatter microcolonies compared with MG1655 and ATCC 25404, which had more dramatic vertical structures as a result of their enhanced motility. The presence of flagella was also found to be important as *qseB* and *fliA* mutants (which lack flagella) had less biofilm than the isogenic paralyzed *motA* strain (threefold less thickness and 15-fold less surface coverage).

Introduction

A bacterial biofilm is a community of microorganisms attached to a solid surface using extracellular polymeric substances (Branda et al. 2005). Scanning confocal laser microscopy and fluorescence markers such as the green fluorescence protein (GFP) have been used to show that biofilm communities are non-homogenous as a consequence of rhamnolipid synthesis, growth, or motility phenotypes. However, the relationship of these phenotypes to architecture has not been elucidated (Boles et al. 2004; Werner et al. 2004; Lequette and Greenberg 2005). This complex organization allows cells to respond to different conditions such as temperature (Pham et al. 2004) and the presence of antimicrobials (Szomolay et al. 2005). These robust communities cause health problems such as respiratory, urinary track, and ear infections (Potera 1999) as well as industrial problems such as corrosion (Elvers and Lappin-Scott 2000).

This non-homogeneity in biofilms led us to investigate the relationship between biofilm architecture and cell phenotype. *Pseudomonas aeruginosa*, for example, during biofilm development, exhibits mushroom-like structures which have been attributed to stress forces conditions (Stoodley et al. 1999), substrate gradients (Chang et al. 2003), and differences in gene expression (Espinosa-Urgel 2003). These mushroom structures form channels for nutrient and waste flow (Davey et al. 2003). The scrutiny of *Escherichia coli* biofilm structure is not as developed as that of *P. aeruginosa* because of its usually poor biofilm formation in the absence of conjugation plasmids (Ghigo 2001; Reisner et al. 2003).

In the absence of a conjugation plasmid, type 1 fimbriae expression have been reported to be important for biofilm formation in regard to initial cell attachment (Pratt and Kolter 1998), and motility is essential for biofilm formation, probably for overcoming the electrostatic repulsion of cells and surfaces (Pratt and Kolter 1998; Walker et al. 2004). However, the role of motility on biofilm maturation and its effect on architecture have not been elucidated, as there is not a clear report that relates motility and mature biofilm formation in *E. coli* (Reisner et al. 2003; Lazazzera 2005). Although studies on DNA microarrays of *E. coli* cells have not found to date a significant difference in flagella expression during biofilm development (Schembri et al. 2003; Beloin et al. 2004; Ren et al. 2004), other

T. K. Wood (✉) · A. F. González Barrios · M. Herzberg · J. Lee
Departments of Chemical Engineering and Biology,
Texas A & M University,
College Station, TX 77843-3122, USA
e-mail: thomas.wood@chemail.tamu.edu
Tel.: +1-979-8621588
Fax: +1-979-8456884

studies have shown that motility genes are repressed in *P. aeruginosa* in a 5-day biofilm and in *Bacillus subtilis* biofilms after 8, 12, and 24 h (Whiteley et al. 2001; Stanley et al. 2003).

The aim of this study was to investigate the role of motility in biofilm architecture using a series of *E. coli* strains with differences in motility. We chose to use continuous flow cells so that the biofilms could be compared rigorously on a consistent basis and used software that helps to avoid microscopic artifacts (Heydorn et al. 2002). This is the first report that relates motility and *E. coli* mature biofilm formation.

Materials and methods

Bacterial strains and growth media The *E. coli* strains and plasmids are listed in Table 1. Biofilm flow chamber studies were performed using strains harboring the GFP plasmid pCM18 (Hansen et al. 2001) to visualize the biofilm. Minimal medium M9 with 0.4% casamino acids and 0.4% glucose (M9C glu) (Rodriguez and Tait 1983) was used to assay motility gene expression and for the flow chamber experiments. For plasmid selection, antibiotics were added to the cultures at 100 μg/ml for ampicillin, 50 μg/ml for kanamycin, and 30 μg/ml for chloramphenicol.

Promoter transcriptional assays MG1655, ATCC 25404, BW25113, and JM109 with the plasmid-based (Table 1) transcriptional reporters *qseB::lacZ, flhD*::*lacZ*, *fliA*::*lacZ*, *fliC*::*lacZ*, and *motA*::*lacZ* (Sperandio et al. 2002) were cultured overnight in LB ampicillin, diluted 1:100 in LB media, and grown to exponential phase to a turbidity of 1 at 600. Once cells reached this OD, they were centrifuged for 5 min at 4°C at 13,800×*g*, resuspended in 750 μl of Tris–ethyl diamine tetraacetic acid–phenyl methyl sulphonyl fluoride buffer, and sonicated in two intervals of 15 s at 10 W. The samples were assayed for β-galactosidase activity using *o*-nitrophenyl-β-galactopyranoside (Sigma, St Louis, USA) as described previously (Wood and Peretti 1991). All activities were calculated based on a protein concentration of 0.24 mg protein/ml/OD_{600} unit (Fishman et al. 2005). Each experiment was performed twice with two independent cultures for each strain in M9C glu.

Flow chamber biofilm experiments and image analysis M9C glu medium was supplemented with erythromycin to maintain the green fluorescent plasmid pCM18 at 120 μg/ml for MG1655, ATCC 25404, DH5α, and MG1655 *motA* and 300 μg/ml for JM109 and BW25113. Biofilms were formed at 37°C in a continuous flow chamber (BST model FC81, Biosurface Technologies, Bozeman, MT) with chamber dimensions of 47.5×12.7 mm with a 1.6-mm gap between the surfaces by inoculating 1.1 to 4.35×10^7 cells/ml. The flow chambers were cleaned with 95% alcohol and sterilized by autoclaving. The flow cell contains a standard glass microscope slide on one side and a plastic cover slip on the other side. An overnight culture was diluted 1/100 in the M9C glu medium. A diluted overnight culture (turbidity of 0.05) was allowed to flow into the flow chamber for 2 h at a flow rate of 10 ml/h (in

Table 1 *E. coli* strains and plasmids used. Amp^R and Em^R are ampicillin and erythromycin resistance, respectively

Strains and plasmids	Genotype	Source or reference
Strains		
K12	Wild type	ATCC 25404
K12 MG1655	F-lambda- *ilvG- rfb*-50 *rph*-1	(Blattner et al. 1997)
K12 BW25113	$lacI^q rrnB_{T14}$ Δ$lacZ_{WJ16}$ hsdR514 Δ*araBA*-D_{AH33} Δ*rhaBAD*$_{LD78}$	(Datsenko and Wanner 2000)
JM109	*recA1 supE44 endA1 hsdR17 gyrA96 relA1 thi Δ(lac-proAB)* F'*[traD36 proAB*$^+$*lacI*^{q}*lacZΔM15]*	(Yanisch-Perron et al. 1985)
DH5α	*LuxS supE44* Δ*lacU169*, (ϕ80 *lacZ*ΔM15) *hsdR17*, *recA1*, *endA1*, *gyrA96*, *thi-1*, *relA1*	(Sambrook et al. 1989)
MG1655 *motA*	K12 Δ*motA::*Tn*5*Kan-2	(Kang et al. 2004)
MG1655 *qseB*	K12 Δ*qseB::*Tn*5*Kan-2	(Kang et al. 2004)
MG1655 *fliA*	K12 Δ*fliA::*Tn*5*Kan-2	(Kang et al. 2004)
Plasmids		
pCM18	Em^R, pTRKL2-P_{CP25}-RBSII-*gfp*mut3*-T_0-T_1 (GFP plasmid for visualizing biofilm)	(Hansen et al. 2001)
pVS159	Amp^R, *qseB*::*lacZ* in pRS551	(Sperandio et al. 2002)
pVS176	Amp^R, *motA*::*lacZ* in pRS551	(Sperandio et al. 2002)
pVS175	Amp^R, *fliC*::*lacZ* in pRS551	(Sperandio et al. 2002)
pVS183	Amp^R, *fliAehK12*::*lacZ* in pRS551	(Sperandio et al. 2002)
pVS182	Amp^R, *flhD::lacZ* in pRS551	(Sperandio et al. 2002)

laminar flow) before fresh medium was added at the same flow rate; this culture was aerated by stirring the feed flask. The biofilm development was monitored at 24 h (MG1655 was monitored at 24 and 48 h) using a TCS SP2 scanning confocal laser microscope with a 40× N PLAN L dry objective with correction collar and numerical aperture of 0.55 (Leica Microsystems, Heidelberg, Germany). The ATCC 25404 and BW25113 flow cells were performed in duplicate.

Color confocal flow chamber images were converted to gray scale using Image Converter (Neomesh Microsystems, Wainuiomata, Wellington, New Zealand). Biomass, surface coverage, surface roughness, and mean thickness were determined using COMSTAT image-processing software (Heydorn et al. 2000) written as a script in Matlab 5.1 (The MathWorks) equipped with the image processing toolbox. Thresholding was fixed for all image stacks, and 25 planar images were processed for each position; in total, nine positions with 25 images were obtained for each strain so a total of 1800 images were analyzed. Values are means of data from the different positions at the same time point, and standard deviations were calculated based on these mean values for each position. Simulated three-dimensional images were obtained using IMARIS (Bitplane, Zurich, Switzerland). Twenty-five planar images were processed for each three-dimensional image.

Motility assays LB overnight cultures were used to assay motility in plates containing 1% tryptone and 0.25% NaCl and 0.3% agar. The motility halos were measured at 8 h (Sperandio et al. 2002). Three plates were used to evaluate the motility in each strain, and the experiments were conducted with two independent cultures.

Results

Biofilm architecture As different strains have been used to study *E. coli* biofilm formation (Pratt and Kolter 1998; Ren et al. 2001; Beloin et al. 2004; Ren et al. 2004), we investigated the impact of strain on biofilm architecture using flow chambers. The two wild-type strains ATCC 25404 and MG1655 formed good biofilms, as their architecture was that of a mature biofilm (Reisner et al. 2003), and displayed few differences for the COMSTAT parameters evaluated (Table 2, Figs. 1a and 2a). For these two strains, the most common parameter used for describing biofilm literature (Heydorn et al. 2000), mean thickness, was very similar (42±6 and 44±6 μm), as were surface coverage (21±8 and 34±13%) and the amount of biomass (24±10 and 11±8 $\mu m^3/\mu m^2$). The roughness coefficient, which provides a measure of how much the thickness of the biofilm varies (Heydorn et al. 2000), is higher in ATCC 25404 compared with MG1655 (0.51±0.10 vs 0.20±0.09); therefore, MG1655 is more heterogeneous than ATCC 25404. ATCC 25404 and MG1655 display cylindrical towers and scattered structures on the surface (Figs. 1a and 2a) which resemble the mushroom structures reported for *P. aeruginosa* (Lequette and Greenberg 2005) showing liquid channels inside the biofilm. However, different from mushrooms, the structures displayed by ATCC 25404 and MG1655 are not flat at the top. A more detailed view of the biofilm structure for each strain studied here can be seen on http://cheweb.tamu.edu/orgs/groups/Wood/biofilm%20architecture.htm.

Table 2 COMSTAT analysis of the *E. coli* biofilms formed in continuous flow cells with M9C glu containing erythromycin (concentrations in Materials and methods section) after 24 h, and motility of the *E. coli* strains at 8 h. One standard deviation is shown from two independent cultures

Strain	Mean thickness[a] (μm)	Surface coverage[a] (%)	Biomass[a] ($\mu m^3/\mu m^2$)	Roughness coefficient[a]	Motility (cm)
ATCC 25404	42±6	21±8	24±10	0.5±0.1	0.6±0.05
MG1655	44±6	34±13	11±8	0.20±0.09	0.9±0.1
BW25113	13±5	2±1	4±1	1.0±0.4	0.16±0.05
JM109	15±8	50±20	13±6	1.0±0.4	0.12±0.03
DH5α	10±4	41±11	8±3	1.0±0.2	ND
MG1655 *motA*	16±6	58±4	12±4	0.7±0.1	ND
MG1655 *qseB*	6±2	3±2	4±1	1±0.1	ND
MG1655 *fliA*	5±2	5±2	3±1	1±0.1	ND

ND Halo not detected
[a](Heydorn et al. 2000)

BW25113 (Datsenko and Wanner 2000), whose genotype (Table 1) does not exhibit mutations in genes related to biofilm formation reported to date, was not able to form a robust biofilm in minimal medium, as there was a reduction of thickness (threefold), biomass (5.4-fold), and surface coverage (ninefold) compared with ATCC 25404 (Table 2, Fig. 1b). JM109 and DH5α displayed a similar biofilm architecture with each other but different from that of ATCC 25404 and MG1655 (Fig. 1c,d) in that these two strains cover the glass surface more efficiently (substratum coverage is twofold higher), and JM109 and DH5α displayed smoother colonies compared with ATCC 25404 and MG1655 (Figs. 1a and 2a). The mean thickness (15±8 and 10±4 μm) and total biomass values (13±6 and 8±3 $\mu m^3/\mu m^2$) show fewer cells accumulated for JM109 and DH5α, respectively, compared with ATCC 25404 (42±6 μm and 24±10 $\mu m^3/\mu m^2$, respectively) and MG1655 (44±6 μm and 11±8 $\mu m^3/\mu m^2$, respectively).

The ATCC 25404 and BW25113 flow cell experiments were duplicated and we obtained consistent COMSTAT and architecture results for both. For example, the COMSTAT mean thickness for ATCC 25404 (38±12 μm vs 47±5 μm) and for BW25113 (16±2 μm vs 10±2 μm) were reproducible.

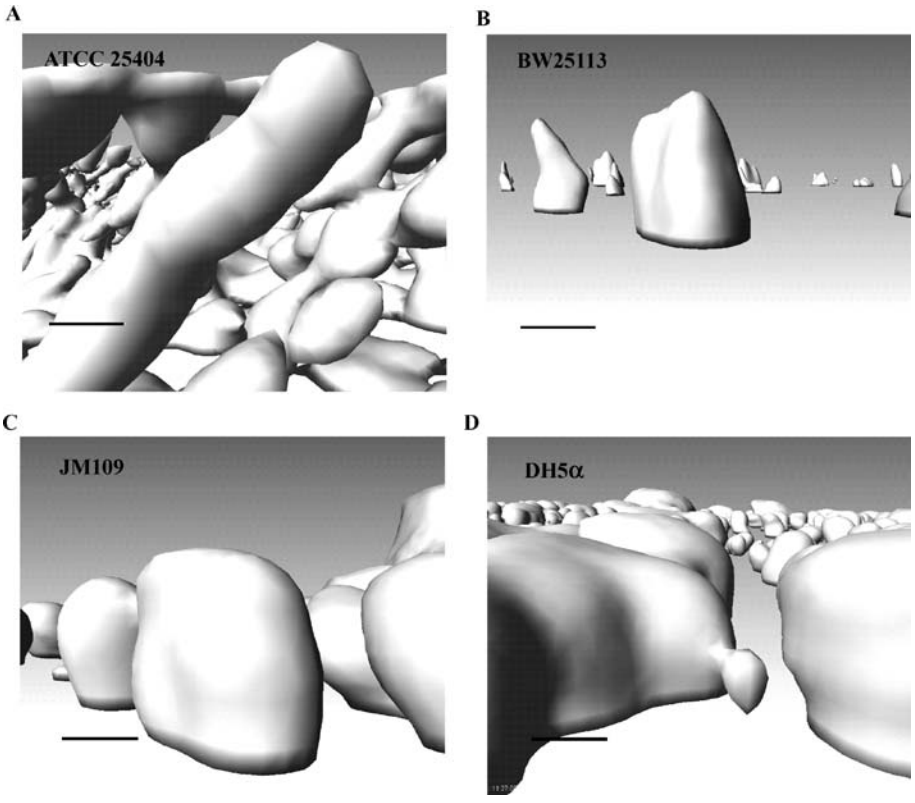

Fig. 1 Biofilm architecture for ATCC 25404 (**a**), BW25113 (**b**), JM109 (**c**), and DH5α (**d**) obtained in continuous flow chambers with M9C glu after 24 h. Scale bar represents 5 μm

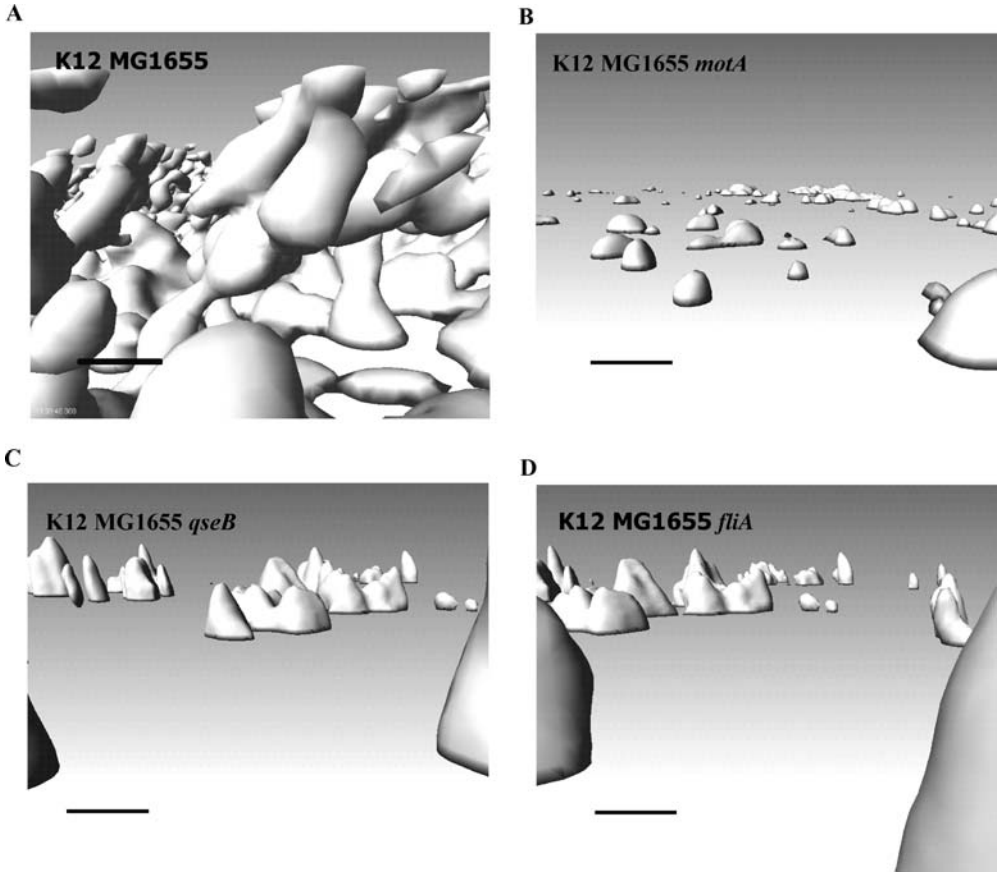

Fig. 2 Biofilm architecture for MG1655 (**a**), MG1655 *motA* (**b**), MG1655 *qseB* (**c**), and MG1655 *fliA* (**d**) obtained in continuous flow chambers after 24 h with M9C glu and erythromycin for mutants. Scale bar represents 5 μm

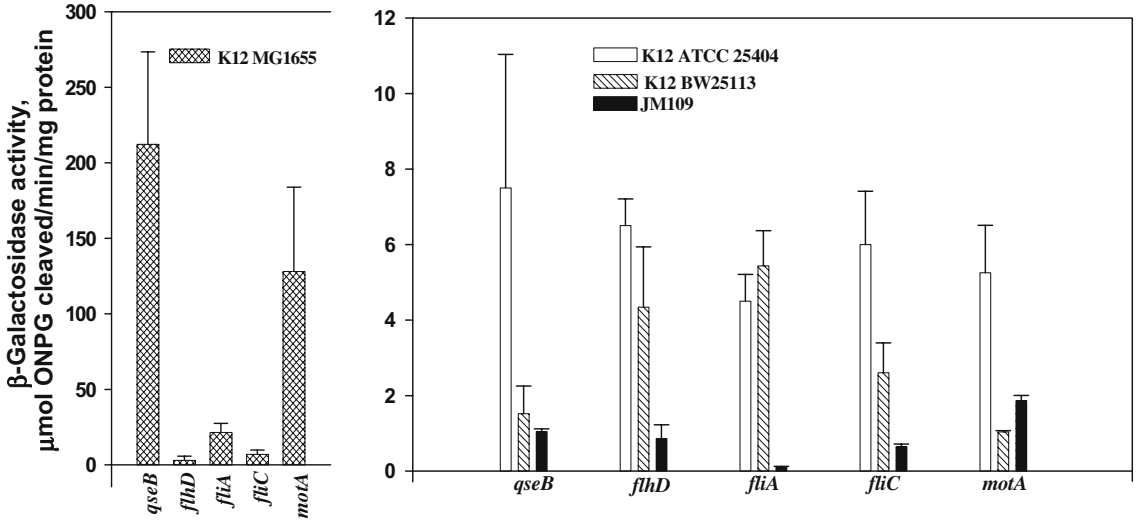

Fig. 3 Transcription of *qseB*::*lacZ*, *flhD*::*lacZ*, *fliA*::*lacZ*, *fliC*::*lacZ*, and *motA*::*lacZ* in MG1655, ATCC 25404, BW25113, and JM109 in M9C glu. The experiment was performed with two independent cultures, and one standard deviation is shown. Note the different *Y*-axis *scales* used in the two panels

Motility It is established that motility plays an important role in biofilm development of *E. coli* (Pratt and Kolter 1998) although the presence of a conjugation plasmid overrides the dependence on motility (Reisner et al. 2003). We therefore tested the motility of the strains and found that MG1655 and ATCC 25404 displayed the highest motility (MG1655 is slightly more motile than ATCC 25404) as MG1655 displayed six- and eightfold more motility than JM109 and BW25113, respectively (Table 2). There was no motility for DH5α, and the paralyzed strain MG1655 *motA* was non-motile, as expected.

Using transcriptional reporters, we found that the differences in motility are due to the differences in flagella gene expression (Fig. 3). MG1655 had the highest quorum sensing flagella regulon expression (*qseB*) (Sperandio et al. 2002) which was 28-fold greater than ATCC 25404, 139-fold greater than BW25113, and 209-fold greater than JM109. This difference in *qseB* expression was also reflected in the expression of *motA* (encodes the motor torque generator for flagella movement) (Chilcott and Hughes 2000) as *motA* expression for MG1655 was higher compared with ATCC 25404 (24-fold), BW25113 (123-fold), and JM109 (68-fold).

ATCC 25404 had high *qseB* transcription compared with BW25113 and JM109, which explains the differences in the motility phenotype between these strains. These differences in the motility phenotype were also reflected in the biofilm architecture. The strains that were highly motile had high flagella expression (MG1655 and ATCC 25404) and displayed vertical biofilm structures, whereas the strains with low motility, as a consequence of lower flagella gene expression (BW25113, JM109, and DH5α), displayed smoother microcolonies (Fig. 1).

Motility vs flagella To determine if the difference in biofilm architecture is related to motility or flagella assembly, *qseB* and *fliA* isogenic mutants deficient in flagella assembly were compared with the paralyzed *motA* mutant which has an intact flagella assembly (Chilcott and Hughes 2000) using flow cells (Table 2; Fig. 2b–d). The deletion of *qseB* and *fliA* leads to a dramatic decrease in biomass (sixfold for *qseB* and eightfold for *fliA*), surface coverage (11-fold for *qseB* and sevenfold for *fliA*), and mean thickness (sevenfold for *qseB* and ninefold for *fliA*) compared with the isogenic MG1655 wild-type strain. In contrast, the reductions in biomass, surface coverage, and mean thickness were less severe for *motA* mutant. The biofilm architecture of the *motA* mutant (Fig. 2b) was similar to the structures exhibited by *E. coli* JM109 and *E. coli* DH5α (Fig. 1c,d), which also display poor motility (Table 2). This similarity was corroborated with COMSTAT, as biomass, surface coverage, and mean thickness were similar for these three strains (Table 2); for example, mean thickness was similar for JM109 (15±8 μm), DH5α (10±4 μm), and the *motA* mutant (16±6 μm). Hence, *E. coli* biofilm architecture is impacted both by motility and the presence of flagella. Growth was not altered after deleting *qseB*, *fliA*, and *motA* so the changes in the biofilm are not a result of growth rate differences. The specific growth rates in M9C glu were 0.96±0.004/h for MG1655, 0.99±0.01/h for MG1655 *qseB*, 1.00±0.04/h for MG1655 *fliA*, and 0.97±0.01/h for the *motA* mutant.

Discussion

In this work, we show that there are differences in biofilm architecture for the *E. coli* strains MG1655, ATCC 25404, BW25113, JM109, and DH5α. Differences in flagella expression were also clearly demonstrated for the strains, and the level of expression of the quorum sensing master flagella regulon *qseB* (MG1655>ATCC 25404>BW25113>JM109, Fig. 3) agrees with the observed cell motility (MG1655>ATCC 25404>BW25113>JM109>DH5α, Table 2).

We hypothesize that the differences in mature biofilm architecture are caused by these differences in motility. High motility leads to vertical structures displayed by MG1655 and ATCC 25404 (Figs. 1a and 2a), and when motility is reduced, smoother colonies are formed like the structures exhibited by JM109 and DH5α (Fig. 1c,d). We also determined that the differences in architecture are caused by flagella rotation as well as the by the presence of the flagella themselves. The deletion of *qseB* or *fliA* affects cell attachment and motility with the result that there is a dramatic decrease in biofilm formation, while deletion of *motA* (which affects only motility) results in less severe defects in the biofilm (Table 2, Fig. 2). Hence, we report a strong relationship between motility, flagella, and biofilm architecture in mature *E. coli* biofilms.

Unexpectedly, the difference in *qseB* expression was not reflected in the expression of *flhD* and *fliA* for BW25113 and of *flhD*, *fliA*, and *fliC* for MG1655 (Fig. 3). Out of the genes whose expression was measured, *motA* is the one that reflected best the expression of *qseB* (Fig. 3). This also suggests that the movement of flagella via *motA* may play the most important role in tower formation for mature biofilm architecture (for these five motility genes) (cf., MG1655 vs MG1655 *motA*, Fig. 2a vs b).

Acknowledgements We thank A. Heydorn from the Technical University of Denmark for kindly providing COMSTAT, S. Molin from the Technical University of Denmark for sending plasmid pCM18, and J. Kaper from the University of Maryland for sending plasmids pVS159, pVS176, pVS175, pVS182, and pVS183.

References

Beloin C, Valle J, Latour-Lambert P, Faure P, Kzreminski M, Balestrino D, Haagensen JAJ, Molin S, Prensier G, Arbeille B, Ghigo J-M (2004) Global impact of mature biofilm lifestyle on *Escherichia coli* K-12 gene expression. Mol Microbiol 51: 659–674

Blattner FR, Plunkett G III, Bloch CA, Perna NT, Burland V, Riley M, Collado-Vides J, Glasner JD, Rode CK, Mayhew GF, Gregor J, Davis NW, Kirkpatrick HA, Goeden MA, Rose DJ, Mau B, Shao Y (1997) The complete genome sequence of *Escherichia coli* K-12. Science 277:1453–1462

Boles BR, Thoendel M, Singh PK (2004) Self-generated diversity produces "insurance effects" in biofilm communities. Proc Natl Acad Sci USA 101:16630–16635

Branda SS, Vik Å, Friedman L, Kolter R (2005) Biofilms: the matrix revisited. Trends Microbiol 13:20–26

Chang I, Gilbert ES, Eliashberg N, Keasling JD (2003) A three-dimensional stochastic simulation of biofilm growth and transport-related factors that affect structure. Microbiol 149:2859–2871

Chilcott GS, Hughes KT (2000) Coupling of flagellar gene expression to flagellar assembly in *Salmonella enterica serovar typhimurium* and *Escherichia coli*. Microbiol Mol Biol Rev 64:694–708

Datsenko KA, Wanner BL (2000) One-step inactivation of chromosomal genes in *Escherichia coli* K-12 using PCR products. Proc Natl Acad Sci USA 97:6640–6645

Davey ME, Caiazza NC, O'Toole GA (2003) Rhamnolipid surfactant production affects biofilm architecture in *Pseudomonas aeruginosa* PAO1. J Bacteriol 185:1027–1036

Elvers KT, Lappin-Scott HM (2000) Biofilms and biofouling, 2nd edn. Academic, San Diego, California

Espinosa-Urgel M (2003) Resident parking only: rhamnolipids maintain fluid channels in biofilms. J Bacteriol 185:699–700

Fishman A, Tao Y, Rui L, Wood TK (2005) Controlling the regiospecific oxidation of aromatics via active site engineering of toluene *para*-monooxygenase of *Ralstonia pickettii* PKO1. J Biol Chem 280:506–514

Ghigo J-M (2001) Natural conjugative plasmids induce bacterial biofilm development. Nature 412:442–445

Hansen MC, Palmer RJ Jr, Udsen C, White DC, Molin S (2001) Assessment of GFP fluorescence in cells of *Streptococcus gordonii* under conditions of low pH and low oxygen concentration. Microbiol 147:1383–1391

Heydorn A, Ersboll B, Kato J, Hentzer M, Parsek MR, Tolker-Nielsen T, Givskov M, Molin S (2002) Statistical analysis of *Pseudomonas aeruginosa* biofilm development: impact of mutations in genes involved in twitching motility, cell-to-cell signaling, and stationary-phase sigma factor expression. Appl Environ Microbiol 68:2008–2017

Heydorn A, Nielsen AT, Hentzer M, Sternberg C, Givskov M, Ersbøll BK, Molin S (2000) Quantification of biofilm structures by the novel computer program COMSTAT. Microbiol 146:2395–2407

Kang Y, Durfee T, Glasner JD, Qiu Y, Frisch D, Winterberg KM, Blatnner FR (2004) Systematic mutagenesis of the *Escherichia coli* genome. J Bacteriol 186:4921–4930

Lazazzera BA (2005) Lessons from DNA microarray analysis: the gene expression profile of biofilms. Curr Opin Microbiol 8:222–227

Lequette Y, Greenberg EP (2005) Timing and localization of rhamnolipid synthesis gene expression in *Pseudomonas aeruginosa* biofilms. J Bacteriol 187:37–44

Pham TH, Webb JS, Rehm BHA (2004) The role of polyhydroxyalkanoate biosynthesis by *Pseudomonas aeruginosa* in rhamnolipid and alginate production as well as stress tolerance and biofilm formation. Microbiol 150:3405–3413

Potera C (1999) Forging a link between biofilms and disease. Science 283:1837–1839

Pratt LA, Kolter R (1998) Genetic analysis of *Escherichia coli* biofilm formation: roles of flagella, motility, chemotaxis and type I pili. Mol Microbiol 30:285–293

Reisner A, Haagensen JAJ, Schembri MA, Zechner EL, Molin S (2003) Development and maturation of *Escherichia coli* K-12 biofilms. Mol Microbiol 48:933–946

Ren D, Bedzyk LA, Thomas SM, Ye RW, Wood TK (2004) Gene expression in *Escherichia coli* biofilms. Appl Microbiol Biotechnol 64:515–524

Ren D, Sims JJ, Wood TK (2001) Inhibition of biofilm formation and swarming of *Escherichia coli* by (5*Z*)-4-bromo-5-(bromomethylene)-3-butyl-2(5*H*)-furanone. Environ Microbiol 3:731–736

Rodriguez RL, Tait RC (1983) Recombinant DNA techniques: an introduction. Benjamin/Cummings Publishing, Menlo Park, CA

Sambrook J, Fritsch EF, Maniatis T (1989) Molecular cloning, a laboratory manual, 2nd ed. Cold Spring Harbor Laboratory, Cold Spring Harbor, NY

Schembri MA, Kjærgaard K, Klemm P (2003) Global gene expression in *Escherichia coli* biofilms. Mol Microbiol 48:253–267

Sperandio V, Torres AG, Kaper JB (2002) Quorum sensing *Escherichia coli* regulators B and C (QseBC): a novel two-component regulatory system involved in the regulation of flagella and motility by quorum sensing in *E. coli*. Mol Microbiol 43:809–821

Stanley NR, Britton RA, Grossman AD, Lazazzera BA (2003) Identification of catabolite repression as a physiological regulator of biofilm formation by *Bacillus subtilis* by use of DNA microarrays. J Bacteriol 185:1951–1957

Stoodley P, Lewandowski Z, Boyle JD, Lappin-Scott HM (1999) The formation of migratory ripples in a mixed species bacterial biofilm growing in turbulent flow. Environ Microbiol 1:447–455

Szomolay B, Klapper I, Dockery J, Stewart PS (2005) Adaptative responses to antimicrobial agents in biofilms. Environ Microbiol 7:1186–1191

Walker SL, Redman JA, Elimelech M (2004) Role of cell surface lipopolysaccharides in *Escherichia coli* K12 adhesion and transport. Langmuir 20:7736–7746

Werner E, Roe F, Bugnicourt A, Franklin MJ, Heydorn A, Molin S, Pitts B, Stewart PS (2004) Stratified growth in *Pseudomonas aeruginosa* biofilms. Appl Environ Microbiol 70:6188–6196

Whiteley M, Bangera MG, Bumgarner RE, Parsek MR, Teitzel GM, Lory S, Greenberg EP (2001) Gene expression in *Pseudomonas aeruginosa* biofilms. Nature 413:860–864

Wood TK, Peretti SW (1991) Effect of chemically-induced, cloned-gene expression on protein synthesis in *E. coli*. Biotechnol Bioeng 38:397–412

Yanisch-Perron C, Vieira J, Messing J (1985) Improved M13 phage cloning vectors and host strains: nucleotide sequences of the M13mp18 and pUC19 vectors. Gene 33:103–119